

# Design of jet-driven, radiative-blast-wave experiments for 10 kJ class lasers

R.P. Drake · J.P. Knauer

Received: 7 June 2008 / Accepted: 28 October 2008 / Published online: 25 November 2008  
© Springer Science+Business Media B.V. 2008

**Abstract** We discuss the design of jet-driven, radiative-blast-wave experiments for a 10 kJ class pulsed laser facility. The astrophysical motivation is the fact that jets from Young Stellar Objects are typically radiative and that the resulting radiative bow shocks produce complex structure that is difficult to predict. To drive a radiative bow shock, the jet velocity must exceed the threshold for strong radiative effects. Using a 10 kJ class laser, it is possible to produce such a jet that can drive a radiative bow shock in gas that is dense enough to permit diagnosis by x-ray radiography. We describe the design and simulations of such experiments. The basic approach is to shock the jet material and then accelerate it through a collimating hole and into a Xe ambient medium. We identify issues that must be addressed through experimentation or further simulations in order to field successful experiments.

**Keywords** Jets · Shock waves: radiative

## 1 Introduction

Very young stars typically produce supersonic jets, which drive bow shocks into the surrounding, ambient medium. It became clear in the 1980s that such jets are associated with bright knots known historically, for spectroscopic reasons,

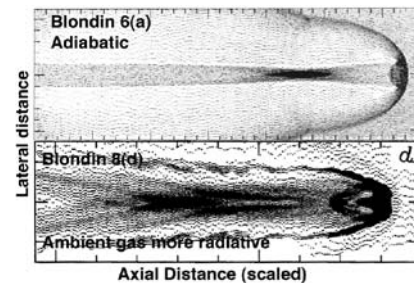


**Fig. 1** Radiative jets, adapted from the paper by Blondin et al. *Top*: shows an adiabatic case without radiative cooling. *Bottom*: a case with much stronger cooling in the ambient gas than in the jet, like the proposed experiment

as Herbig-Haro objects. These bright knots are typically distributed along the jet. Subsequent observations, reviewed by Reipurth (Reipurth and Bally 2001) showed that the jets and the regions they affect are highly structured. Hubble Space Telescope observations have since revealed (Bally et al. 2002) “knots, filaments, small-scale bow shocks, and a complex velocity field.” The driven shocks are necessarily radiative, as is discussed in the recent review by Dal Pino (2005), whose references include the large body of simulation work on these systems. Simulations indicate that this strong radiative cooling has a dramatic impact on the structure of jets. The present paper presents and discusses a design for an experiment to produce a jet that drives a radiative bow shock, intended for specific application to the Omega EP laser facility (Boehly et al. 1995) but also applicable in general to 10 kJ class, pulsed laser facilities.

Figure 1 shows an example of such shocks, from the classic Astrophysical Journal paper by Blondin et al. (1990). The bottom portion of this figure shows the case that we propose to produce and study, in which strong radiative effects are present in the shocked, ambient gas. The radia-

R.P. Drake (✉)  
University of Michigan, Ann Arbor, USA  
e-mail: rpdrake@umich.edu

J.P. Knauer  
Laboratory for Laser Energetics, University of Rochester,  
Rochester, USA

tive cooling collapses the blast wave around the jet and creates more complicated spatial structure through the action of various instabilities, notably including Kelvin-Helmholtz instabilities because of shear between the jet flow and the ambient medium. The structures along the edges of the jet in Fig. 1 were attributed to Kelvin-Helmholtz instabilities. Such structures have not been seen in non-radiative jet experiments (Foster et al. 2005; Rosen et al. 2005). When there is strong cooling of the shocked gas, Blondin et al. attribute some of the structure near the head of the jet to the Vishniac instability (Vishniac 1983). They attribute other structure, behind the head of the jet, to conical shocks launched dynamically. A large number of subsequent papers have explored jet structure under various assumptions, including for example the effect of Kelvin-Helmholtz in three dimensions (Xu et al. 2000), the effects of pulsations in the jet source combined with magnetic fields (Gardiner et al. 2000; O'Sullivan and Ray 2000), and the consequences of different types of cooling (Moraghan et al. 2006). Such simulations do not easily obtain sufficient resolution to resolve the details (Plewa 1993; Rosen and Smith 2004). At the present time there are many simulations of radiative jets, all showing complex structure, but typically differing regarding the details of such structure, even when the nominal physical assumptions are the same. The role for experiments is thus to observe the structure produced under well-defined experimental conditions in which radiation is important. This is the need that the present design addresses.

The experiment design discussed here follows a substantial body of jet-related research in the high-energy-density laboratory astrophysics community during the past decade. The first laser-driven jet experiments could produce jets in isolation and observe their radiative collapse using laser-ablated plasma (Farley et al. 1999), or could produce jets whose length did not greatly exceed their diameter by inverting a pin in a target (Foster et al. 2002). Designs for extended, laser-driven, supersonic jets that can penetrate an ambient medium involve the expansion and acceleration of a shocked plasma down a collimating tube. These were developed by E.C. Harding and R.P. Drake in a memorandum in 2000, with the first multi-dimensional design simulations being discussed in a memorandum by A.M. Khokhlov in 2001. This led over time to a large team effort, culminating in publications of experimental results by Foster et al. (2005) and Rosen et al. (2005). In work contemporary with this, S. Sublett employed a similar approach and some others in doctoral thesis work (Sublett 2007; Sublett et al. 2007). Similar approaches have since been employed in experiments on the National Ignition Facility (Blue et al. 2005) and in Europe (Loupias et al. 2007a, 2007b). In addition, two alternative approaches to jet formation have been developed. These are the use of wire-ablation plasmas from Z-pinch devices to produce jets (Ciardi et al.

2002; Lebedev et al. 2002, 2004) and the use of ring-shaped laser irradiation of planar surfaces to produce jets (Kasperczuk et al. 2006; Nicolai et al. 2006, 2007). We will refer to the latter objects as “ring jets”. Both of these techniques can also drive the jet into an ambient medium.

In both the Z-pinch and the ring jets the bow shocks must be driven into gas at densities that can be accommodated within a vacuum system, creating a physical system suitable for diagnosis by optical techniques such as interferometry and Schlieren. In contrast, the experiments discussed here would use denser gas within an enclosed target, enabling them to diagnose the dense shocked gas by radiography. This is thus a complementary approach, with some potential advantages in spatial resolution and in the ability to see structure within very dense regions.

## 2 Experiment design

In order to create a radiative bow shock it is necessary that the energy flux due to thermal radiative losses from an optically thick layer of shocked material would exceed the energy flux entering the shocked material. One can express this condition as  $R_r > 1$ , where

$$R_r = \frac{\sigma T_{init}^4}{\rho_o u_s^3 / 2} = \frac{32(\gamma - 1)^4}{(\gamma + 1)^8} \frac{\sigma}{c_v^4} \frac{u_s^5}{\rho_o}, \quad (1)$$

in which  $u_s$  is the shock velocity,  $\sigma$  is the Stefan-Boltzmann constant,  $\rho_o$  is the mass density of the unshocked material,  $\gamma$  is the polytropic index appropriate to the shock transition and the post-shock electron temperature,  $T_{init}$  is (Drake 2005)

$$T_{init} = \frac{2(\gamma - 1) u_s^2}{(\gamma + 1)^2 c_v}, \quad (2)$$

in which  $c_v$  is the specific heat at constant volume of the post shock material, approximately equal to  $(Z + 1)k_B/(Am_p)$  for a fully ionized gas. Here the post-shock level of ionization is  $Z$ , the atomic mass of the shocked material is  $A$ , the proton mass is  $m_p$ , and the Boltzmann constant is  $k_B$ . To exceed the threshold of (1), a shock wave in Xe at 1 atm pressure must propagate above about 50 km/s.

Figure 2 shows the schematic design of the experiment. Its operation is as follows. Three beams of Omega EP irradiate a thin plastic layer on the surface of a mid-Z material (Al or Ti). The resulting ablation pressure shocks and accelerates this material, which moves and expands down a collimating tube, allowing the leading edge to accelerate, before emerging as a jet. This technique has been used previously to produce hydrodynamic jets in foam (Foster et al. 2005; Rosen et al. 2005; Sublett et al. 2007). In our case the jet will emerge into a large volume of Xe gas at 1 atmosphere pressure. So long as the leading edge of the jet is moving above

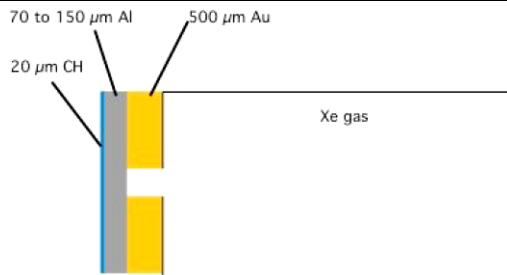


**Fig. 2** Schematic of radiative blast wave target

50 km/s, the shock driven into the Xenon will be strongly radiative and will collapse spatially in consequence.

A principal and unknown limitation on such experiments is that for the immediate future at Omega EP, the available beam smoothing will be by Distributed Phase Plates (DPPs) only. This will produce a larger seed for Rayleigh-Taylor growth than has been present in past Omega-60 radiative shock experiments. The simulations discussed below indicate that the higher laser energy can make up for this, by enabling the acceleration of thicker blocks of material. The question of how much material can be accelerated and to what velocity remains significant for this experiment and will need to be addressed by measurements.

The options for irradiation range from 7.5 kJ at 1 ns to 19.5 kJ at 10 ns. Using a 300 μm spot at 1 ns would produce an irradiance of  $10^{16}$  W/cm<sup>2</sup> while using a 500 μm spot at 10 ns would produce  $10^{15}$  W/cm<sup>2</sup>. These spot sizes were used to determine the laser irradiance for preliminary experimental design, although the availability of DPPs may alter the precise available spot sizes. We simulated these cases in 1D using HYADES, run with settings that reproduce other experiments. HYADES (Larsen and Lane 1994) is a Lagrangian code solving one set of continuity and momentum equations and three energy equations (for electron, ions, and radiation). It was run with multigroup-diffusion radiation transport and with flux-limited thermal conduction for electron transport, with an electron flux limiter of 0.05.

In both cases, a jet velocity above 100 km/s was obtained and endured for tens of ns. Correspondingly, a strongly radiative shock was produced in the Xe, which collapsed spatially into a thin, high-density layer. Figure 3 shows a result, for the lower irradiance at a time of 80 ns. After a period of initial evolution, the basic structure of the system, along the axis, is as follows, starting with the shock and moving toward the laser. There is a layer of dense, shocked Xe that has radiatively cooled and collapsed. A layer of low-density, ablated Al follows. The shocked Xe and ablated Al are at approximately the ram pressure of the shock. Behind this, a drifting clump of relatively dense Al follows. This supplies the momentum to sustain the shock. Its pressure decreases moving away from the shock, with a decrease in both density and temperature. Trailing this layer, beyond a temperature

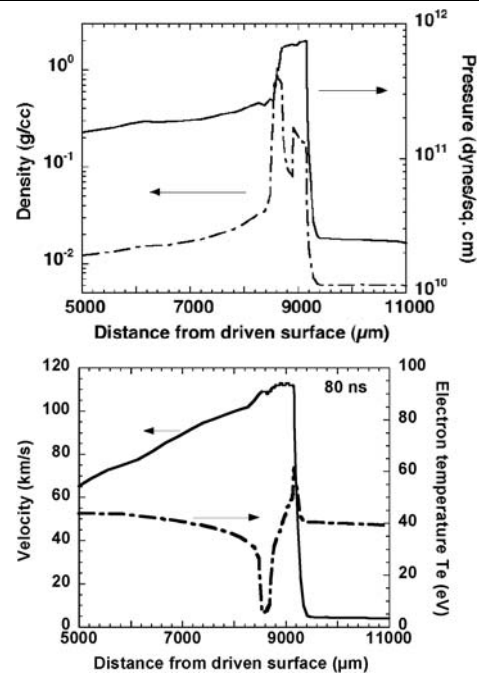


**Fig. 3** Simulated structure of jet and blast wave at 80 ns for the 10 ns laser pulse case. (a) density and pressure (b) velocity and electron temperature

minimum, there is a transition to a lower-pressure, lower-density, freely expanding material that was originally heated and accelerated by the laser. The transition in density originated in the laser ablation front. Earlier in time, the pressure is larger in the laser-heated region; transition in pressure develops during post-laser-pulse cooling.

Some other details about the structure and evolution of the system are worth noting. The transition in pressure at the former ablation front develops quickly (within 10 ns and 1 mm) in the short-pulse case but takes much longer (about 40 ns and 4 mm) in the long-pulse case. The dense layer of shocked Xe is thicker in the figure than would actually be the case with lateral flow. The leading edge of the Al has opposed density and pressure gradients and thus is Rayleigh-Taylor unstable, as is the “working surface” of a typical astrophysical jet. The entire dense structure is about 1 mm thick, much larger than the diagnostic resolution of 10 to 30 μm (to be determined for backlighting on EP). The backlighting might be done either by using a 1 ns pulse with an x-ray framing camera or by using the 80 ps short-pulse beam. Experience gained as the facility is activated will determine the best choice.

The velocity shown in Fig. 3 increases linearly toward the right, as it should for a freely expanding system, and then levels out in the high-pressure region. In the long run, a system like this should develop a reverse shock, where the freely expanding material is slowed to the velocity of the dense material following the accumulated, shocked gas.

After the reverse shock forms, the freely expanding material provides additional energy and momentum to the jet. Enough ambient material must be swept up before this reverse shock will form. This has not happened yet in the case shown. In the case with a 1 ns drive, for which there is less mass in the jet, the reverse shock appears to be forming by 80 ns. The electron temperature structure is complex and reflects the temporal evolution of the system. Moving to the right in Fig. 3, the initial temperature decline is expected for a free expansion. The sharp decrease in temperature as the density increases remains from the initial, limited penetration of the heat front during laser irradiation. The increase in temperature in the Al to the right of the minimum is created by radiative heating from the shocked Xe. The shocked Xe cools radiatively to the left of the shock front, where the temperature is maximum. To the right of the shock front, the temperature has been established by radiative heating. In the actual system, one would expect it to fall off with distance in consequence of radial losses.

There are several detailed design options for the experiment. We tested whether to place a thin gas barrier on the output end of the collimating tube, so that the expansion can occur in vacuum, and found that such a barrier (1  $\mu\text{m}$  plastic) has little effect. The jet material might be Al, Ti, or some other mid-Z metal. Variation of this material or backlighter energy can be used to explore details of the jet morphology. The collimator could be Au as indicated, or another dense material such as W. Past experience has shown that some mass is stripped from the interior of such collimating tubes, and that this can limit the ability to diagnose the interior of the jet. One could line the collimating tube with a lower-Z material to reduce this effect. The precise hole diameter can also vary. The hole needs to stay open while the jet flows through it. With 1 ns laser pulses, 300  $\mu\text{m}$  holes have proven to be sufficient in past experiments. When using a 10 ns laser pulse, a larger hole might be needed.

### 3 Conclusion

We have discussed the design of jet-driven, radiative-blast-wave experiments for a 10 kJ class pulsed laser facility. Using a 10 kJ class laser, it is possible to produce a jet that can drive a radiative bow shock in gas that is dense enough

to permit diagnosis by x-ray radiography. Some issues must be addressed through experimentation or further simulations in order to field successful experiments, including the limits imposed by Rayleigh-Taylor instabilities and the optimum approach to backlighting.

**Acknowledgements** This research was sponsored by the Stewardship Science Academic Alliances program through DOE Research Grants DE-FG52-07NA28058, DE-FG52-04NA00064, and other grants and contracts.

### References

- Bally, J., Heathcote, S., Reipurth, B., Morse, J., Hartigan, P., Schwartz, R.: *Astron. J.* **123**, 2627 (2002)
- Blondin, J.M., Fryxell, B.A., Konigl, A.: *Astrophys. J.* **360**, 370 (1990)
- Blue, B.E., et al.: *Phys. Rev. Lett.* **94** (2005)
- Boehly, T.R., et al.: *Rev. Sci. Instr.* **66**, 508 (1995)
- Ciardi, A., Lebedev, S.V., Chittenden, J.P., Bland, S.N.: *Laser Part. Beams* **20**, 255 (2002)
- Dal Pino, E.M.D.: In: *Fundamentals of Space Environment Science*, p. 908 (2005)
- Drake, R.P.: *Astrophys. Space Sci.* **298**, 49 (2005)
- Farley, D.R., et al.: *Phys. Rev. Lett.* **83**, 1982 (1999)
- Foster, J.M., et al.: *Phys. Plasmas* **9**, 2251 (2002)
- Foster, J.M., et al.: *Astrophys. J. Lett.* **634**, L77 (2005)
- Gardiner, T.A., Frank, A., Jones, T.W., Ryu, D.: *Astrophys. J.* **530**, 834 (2000)
- Kasperczuk, A., et al.: *Phys. Plasmas* **13** (2006)
- Larsen, J.T., Lane, S.M.: *J. Quant. Spectrosc. Radiat. Transfer* **51**, 179 (1994)
- Lebedev, S.V., et al.: *Astrophys. J.* **616**, 988 (2004)
- Lebedev, S.V., et al.: *Astrophys. J.* **564**, 113 (2002)
- Loupias, B., et al.: *Astrophys. Space Sci.* **307**, 103 (2007a)
- Loupias, B., et al.: *Phys. Rev. Lett.* **99** (2007b)
- Moraghan, A., Smith, M.D., Rosen, A.: *Mon. Not. R. Astron. Soc.* **371**, 1448 (2006)
- Nicolai, P., Tikhonchuk, V.T., Kasperczuk, A., Pisarczyk, T., Borodziuk, S., Rohlena, K., Ullschmied, J.: *Phys. Plasmas* **13** (2006)
- Nicolai, P., Tikhonchuk, V.T., Kasperczuk, A., Pisarczyk, T., Borodziuk, S., Rohlena, K., Ullschmied, J.: *Astrophys. Space Sci.* **307**, 87 (2007)
- O'Sullivan, S., Ray, T.P.: *Astron. Astrophys.* **363**, 355 (2000)
- Plewa, T.: *Acta Astron.* **43**, 235 (1993)
- Reipurth, B., Bally, J.: *Ann. Rev. Astron. Astrophys.* **39**, 403 (2001)
- Rosen, A., Smith, M.D.: *Astron. Astrophys.* **413**, 593 (2004)
- Rosen, P.A., et al.: *Astrophys. Space Sci.* **298** (2005)
- Sublett, S.: *Physics and Astronomy*. University of Rochester, Rochester (2007)
- Sublett, S., Knauer, J.P., Igumenshchev, I.V., Frank, A., Meyerhofer, D.D.: *Astrophys. Space Sci.* **307**, 47 (2007)
- Vishniac, E.T.: *Astrophys. J.* **274**, 152 (1983)
- Xu, J.J., Hardee, P.E., Stone, J.M.: *Astrophys. J.* **543**, 161 (2000)